JPn Neuroscience

The Journal of Physiology

J Physiol 591.19 (2013) pp 4807–4825

Kv2 channels regulate firing rate in pyramidal neurons from rat sensorimotor cortex

Dongxu Guan, William E. Armstrong and Robert C. Foehring

Department of Anatomy & Neurobiology, University of Tennessee Health Science Center, 855 Monroe Avenue, Memphis, TN 38163, USA

Key points

- Neurons express many types of potassium channels that are activated by voltage but relatively little is known concerning the division of labour between different channel types in a given cell.
- Our understanding of the functional roles of Kv2 channels has been hindered by the lack of selective pharmacological agents for these channels.
- We manipulated Kv2 channel expression by transfecting pyramidal neurons with wild-type and pore mutant channels.
- We found that reduction in functional Kv2 channels led to slower firing rates, reduced gain of firing and increased spike frequency adaptation.
- We hypothesize that Kv2 channels regulate firing by controlling membrane potential during the inter-spike interval, which in turn regulates availability of voltage-gated sodium channels.

Abstract The largest outward potassium current in the soma of neocortical pyramidal neurons is due to channels containing Kv2.1 α subunits. These channels have been implicated in cellular responses to seizures and ischaemia, mechanisms for intrinsic plasticity and cell death, and responsiveness to anaesthetic agents. Despite their abundance, knowledge of the function of these delayed rectifier channels has been limited by the lack of specific pharmacological agents. To test for functional roles of Kv2 channels in pyramidal cells from somatosensory or motor cortex of rats (layers 2/3 or 5), we transfected cortical neurons with DNA for a Kv2.1 pore mutant (Kv2.1W365C/Y380T: Kv2.1 DN) in an organotypic culture model to manipulate channel expression. Slices were obtained from rats at postnatal days (P7-P14) and maintained in organotypic culture. We used biolistic methods to transfect neurons with gold 'bullets' coated with DNA for the Kv2.1 DN and green fluorescent protein (GFP), GFP alone, or wild type (WT) Kv2.1 plus GFP. Cells that fluoresced green, contained a bullet and responded to positive or negative pressure from the recording pipette were considered to be transfected cells. In each slice, we recorded from a transfected cell and a control non-transfected cell from the same layer and area. Whole-cell voltage-clamp recordings obtained after 3–7 days in culture showed that cells transfected with the Kv2.1 DN had a significant reduction in outward current (~45% decrease in the total current density measured 200 ms after onset of a voltage step from –78 to –2 mV). Transfection with GFP alone did not affect current amplitude and overexpression of the Kv2.1 WT resulted in greatly increased currents. Current-clamp experiments were used to assess the functional consequences of manipulation of Kv2.1 expression. The results suggest roles for Kv2 channels in controlling membrane potential during the interspike interval (ISI), firing rate, spike frequency adaptation (SFA) and the steady-state gain of firing. Specifically, firing rate and gain were reduced in the Kv2.1 DN cells. The most parsimonious explanation for the effects on firing is that in the absence of Kv2 channels, the membrane remains depolarized during the

DOI: 10.1113/jphysiol.2013.257253

ISIs, preventing recovery of Na^+ channels from inactivation. Depolarization and the number of inactivated Na^+ channels would build with successive spikes, resulting in slower firing and enhanced spike frequency adaptation in the Kv2.1 DN cells.

(Received 19 April 2013; accepted after revision 18 July 2013; first published online 22 July 2013)
Corresponding author R. C. Foehring: Department of Anatomy & Neurobiology, University of Tennessee Health Science Center, 855 Monroe Avenue, Memphis, TN 38163, USA. Email: rfoehrin@ithsc.edu

Abbreviations aCSF, artificial cerebrospinal fluid; AHP, afterhyperpolarization; AMPA, amino-3-(3-hydroxy-5-methyl-isoxazol-4-yl)propanoic acid; AP, action potential; AP5, (2*R*)-amino-5-phosphonovaleric acid; CPP, 4-(3-phosphonopropyl)piperazine-2-carboxylic acid; Ctl, control; DN, dominant-negative construct; DNQX, 6,7-dinitroquinoxaline-2,3-dione; GFP, green fluorescent protein; HBSS, Hanks buffered saline; HEK, human embryonic kidney; HW, half-width; HMEM, minimal essential medium plus HBSS and saline; IR-DIC, infrared-differential interference contrast; ISI, interspike interval; Kv2.1 DN, non-functional pore mutant Kv2.1 cDNA; Kv2.1 WT, functional wild-type Kv2.1 cDNA; mAHP, medium afterhyperpolarization; MEM, minimal essential medium; MNTB, medial nucleus of the trapezoid body; NMDA, *N*-methyl-D-asparte; NT, non-transfected; R_{in}, input resistance; RMP, resting membrane potential; sAHP, slow afterhyperpolarization; ScTx, ω-stromatoxin; SFA, spike frequency adaptation; TTX, tetrodotoxin; V_{th}, voltage threshold for action potential; WT, wild-type.

Introduction

There are 12 families of α subunits for voltage-gated Kv channels (Kv1–12) and each family includes several members (Coetzee *et al.* 1999). Most neuronal cell types express several different Kv channel subunits yet we have very limited understanding of the functional division of labour between these channels. Our previous work on acutely dissociated neocortical pyramidal cells revealed whole cell currents through channels containing α subunits from the Kv1, Kv2 and Kv7 families, with the Kv2 component being the largest by far (~60% of the total Kv current during large voltage steps: Guan *et al.* 2006, 2007*a*,*b*, 2011*a*,*b*). These cells also express a transient A-type current, mostly due to Kv4.2 and/or Kv4.3 subunits (Norris & Nerbonne, 2010). An additional component of the A-type current is due to Kv1 channels (Guan *et al.* 2006; Norris & Nerbonne, 2010). Kv2.1 subunits are nearly ubiquitous in their expression and most pyramidal cells also express Kv2.2 subunits (Guan *et al.* 2007*b*; Kihira *et al.* 2010). Recent findings suggest that Kv2.1 and Kv2.2 may form heteromeric channels in pyramidal cells (Kihira *et al.* 2010). Kv2.1-containing channels are located on the axonal initial segment (Sarmiere *et al.* 2008) and the soma and first ~50 μm of the apical dendrite of pyramidal cells (Trimmer, 1991; Hwang *et al.* 1993; Guan *et al.* 2007*b*).

The large amplitude of the Kv2-mediated current in pyramidal neurons suggests important functional roles for these channels. Kv2.1 channels are highly regulated by phosphorylation (Misonou *et al.* 2005*a*; Park *et al.* 2008) and have been implicated in cellular responses to seizures and ischaemia (Misonou *et al.* 2004,2005*b*; Mohapatra *et al.* 2009), mechanisms for intrinsic plasticity (Surmeier and Foehring, 2004; Nataraj *et al.* 2010) and cell death (Pal *et al.* 2003), and responsiveness to anaesthetic agents (Kulkarni *et al.* 1996). There have been relatively few studies of the roles of Kv2 channels in regulating neuronal electrical behaviour, however. Such functional studies have been hindered in particular by the lack of selective pharmacological agents for Kv2 channels.

The Kv2-mediated current activates relatively slowly and at depolarized membrane potentials (Murakoshi & Trimmer, 1999; Guan *et al.* 2007*b*). Due to their slow kinetics and depolarized activation range, Kv2 channels would not be expected to contribute to resting membrane potential (RMP), rheobase, or voltage threshold or repolarization of single action potentials (APs) in neocortical pyramidal neurons (Guan *et al.* 2007*b*), although in other cell types Kv2 channels do have an important role in spike repolarization (Blaine & Ribera, 2001; Malin & Nerbonne, 2002). The slow kinetics and persistence of the Kv2 current also suggests that Kv2 channels may regulate repetitive firing, especially at higher frequencies (Du *et al.* 2000; Malin & Nerbonne, 2002; Johnston *et al.* 2008). To reduce Kv2 current, we used biolistic methods to transfect a Kv2.1 pore mutant (Kv2.1W365C/Y380T: Malin & Nerbonne, 2002) that acts as a dominant negative (DN) into neocortical cells in an organotypic slice culture preparation. Our principal finding was that reduction of Kv2 current resulted in slower firing and reduced *f*–*I* gain in pyramidal cells. This was associated with increased spike frequency adaptation (SFA) and a trend towards more depolarized interspike interval (ISIs), which we hypothesize increased inactivation of voltage-gated Na^+ channels, reducing their availability and slowing firing.

Methods

These studies were performed on juvenile rats [Sprague–Dawley, postnatal days 7 (P7-P14)]. All procedures were approved by the Animal Care and Use Committee of the University of Tennessee Health Science

Center and conform to the principles of UK regulations, as described in Drummond (2009). We used an organotypic culture preparation (Stoppini *et al.* 1991, Foehring *et al.* 2011) to maintain cell morphology and the laminar pattern of cortex. We typically isolated acute neocortical slices at P8–10 and maintained the slices in culture for 3–7 days. This allowed us to study neurons at a similar age range to that in our work with acute slices and minimized the development of exuberant excitatory connections in the slice (cf. Dyhrfjeld-Johnsen *et al.* 2010).

Initial surgery

Briefly, the animals were anaesthetized with isofluorane until they were areflexive. After anaesthesia, the animals were decapitated and the brain was removed and held for 30–60 s in ice-cold artificial cerebrospinal fluid (aCSF) with added 1 mM pyruvic acid and 0.6 mM ascorbate. The aCSF contained (in mM): 125 NaCl, 3 KCl, 2 $CaCl_2$, 2 $MgCl_2$, 1.25 NaH_2PO_4, 26 $NaHCO_3$ and 20 glucose (pH 7.4; 310 mosmol l^{-1}). Under sterile conditions, coronal slices of frontoparietal cortex were cut at 250–300 μm using a vibrating tissue slicer (Campden Vibroslice: World Precision Instruments, Sarasota, FL, USA) and transferred to aCSF continuously bubbled with a 95% O_2/5% CO_2 mixture (room temperature).

Organotypic slice culture

Our procedure has previously been published in detail (Foehring *et al.* 2011). All steps were performed under sterile conditions inside an isolation hood. Briefly, we first washed the slices three times in ∼2 ml wash media [minimal essential medium (MEM): Gibco minimal essential medium]. We then transferred the slices to culture medium, which consists of a mixture of 20 ml HMEM (Lonza BioWhittaker Minimal Essential Media plus HBSS and Hepes, no glutamine), 10 ml HBSS (Gibco Hanks buffered saline) and 10 ml horse serum. We then transfered each individual slice to its own mesh insert and placed the mesh insert/slice in culture media in a six-well plate (Foehring *et al.* 2011). Slices were then incubated at 37°C in an incubator for ∼1 h to stabilize the slices before transfection.

Biolistic transfection

Our primary manipulation of Kv2 channels was to transfect cells with cDNA with a form of Kv2.1 with two pore mutations (W365C/Y380T) that acts as a DN construct (Malin & Nerbonne, 2002). The cDNA was a gift from Dr Jeanne Nerbonne (Washington University, St. Louis). The DN and wild-type (WT) constructs were sequenced in their entirety (University of Tennessee Health Science Center Molecular Resource Center) to ensure that no additional mutations were present. Gold 'bullets' (1.6 μm) were coated with cDNA for the Kv2.1 DN together with cDNA for green fluorescent protein (GFP) to transfect the cells and allow their visualization, respectively (Fig. 1*A*). Neuronal transfection was achieved by particle-mediated gene transfer (biolistics) with a Bio-Rad Helios gene gun (50–100 p.s.i. at 3–5 mm distance). The transfected slices were then maintained for 3–7 days *in vitro* using a modification of the techniques of Stoppini *et al.* (1991), as described in Foehring *et al.* (2011). For detailed protocols for making cDNA 'bullets' and using the gene gun, see Foehring *et al.* (2011) and references therein. As controls for the slices transfected with the Kv2.1 DN plus GFP (Kv2.1 DN), we transfected slices with cDNA for GFP alone (GFP), or with WT Kv2.1 plus GFP (Kv2.1 WT). After transfection, we returned the six-well plates with slices/inserts to the incubator.

Slice culture

We cultured the transfected slices under sterile conditions for 3–7 days (37°C, 5% CO_2) in an incubator (Forma Scientific model # 3110, Thermoscientific, Asheville, North Carolina). The culture medium was replaced every other day.

Slice recordings

For organotypic slice recordings, slices were placed in a recording chamber on the stage of an Olympus BX50WI upright microscope and were bathed in aCSF bubbled with 95% O_2/5% CO_2. The aCSF was delivered at 2 ml min^{-1} and heated with an in-line heater (Warner Instruments, Hamden, CT, USA) to 33 ± 1°C. Pyramidal neurons in layers 2, 3 or 5 were visualized with infrared/differential interference contrast (IR-DIC) video microscopy (Dodt & Zieglgansberger 1990; Stuart *et al.* 1993) using a 40× (0.8 NA) Olympus water-immersion objective and an IR-sensitive camera (Olympus OLY-150 or DAGE-MTI). Pyramidal cells were visually identified by the presence of an apical dendrite ascending towards layer 1, numerous dendritic spines and a pear-shaped soma. The cortical layer was determined by cell density and location relative to the pia. Transfected cells were located using epifluorescence with an FITC filter. We switched between IR-DIC and epifluorescence to determine cell type and whether the cell was transfected (cell appeared green and contained a bullet: Fig. 1*B*). Typically, we found 10–100 transfected cells per slice (Fig. 1*A*).

Electrode position was controlled with Sutter ROE-200 manipulators and PC-200 controller or Luiggs-Neumann manipulators and controller. Whole cell patch-clamp recordings were acquired using either an Multiclamp 700A

(Axon Instruments, Union City, CA, USA) or Multiclamp 700B amplifier and PClamp 9 or 10 software. We recorded with borosilicate electrodes (Warner G150F: 3–8 MΩ in the bath) produced with a horizontal electrode puller (Flaming-Brown P-87; Sutter Instruments, Novato, CA, USA). For current clamp recordings, electrodes were filled with a solution containing (in mM): 130.5 $KMeSO_4$, 10 KCl, 7.5 NaCl, 2 $MgCl_2$, 10 Hepes, 2 ATP, 0.2 GTP and 100 μM EGTA. For voltage-clamp experiments, the internal solution contained (in mM) 85 $KMeSO_4$, 55 KOH, 2 $MgCl_2$, 20 Hepes, 6 creatine phosphate, 3 ATP, 0.5 GTP, 10 BAPTA and 0.1 leupeptin (pH 7.22, 285–295 mOsm l^{-1}). Data were collected only from cells that formed a 1 GΩ or tighter seal. Reported voltages were corrected for the measured liquid junction potential (8 mV). For voltage-clamp recordings the internal included 10 mM BAPTA to prevent activation of calcium-dependent K^+ currents and TTX was added to the extracellular aCSF at 0.5 μM to block the Na^+ current.

To study repetitive firing, current-clamp slice recordings were made in the presence of 6,7-dinitro-quinox-aline-2, 3-dione (DNQX, 20 μM) to block α-amino-3-hydroxy-5-methyl-4-isoxazolep-roipionic acid (AMPA) receptors, 2-amino-5-phosphonovaleric acid (AP5, 50 μM) or 3-(2-carboxypiperazin-4-yl)-propyl-1-phosphonic acid (CPP, 5 μM) to block *N*-methyl-D-aspartate (NMDA) receptors, and picrotoxin (100 μM; to block Cl^- channels, including $GABA_A$ receptors) to ensure that studied effects were exerted directly on the cells recorded from.

Immunofluorescence

Following the recordings, we fixed the slice in PBS-buffered 4% paraformaldehyde and 0.2% picric acid for ∼12–34 h at 4°C, then the slices were blocked and placed in a solution of fixative containing sucrose (30%, w/v) for cryoprotection. The slices were freeze thawed to improve antibody penetration in the organotypic slices and then rinsed in PBS and incubated in 2% normal goat serum for 1–2 h to reduce background staining.

Staining was accomplished using the Neuromab (UC Davis, CA, USA) monoclonal Kv2.1 antibody (K89/34) diluted in PBS-TX and 0.5% Triton X-100 (PBS-TX). Following overnight incubation with the primary antibodies (1:200–1:400), the sections were incubated overnight in the secondary antibody (1:200) consisting of goat anti-mouse (GAM)-AlexaFluor 568 conjugate, at 4°C. The sections were rinsed in PBS-TX, mounted on gelatin-coated slides and coverslipped with Vectashield (Vector). Fluorescence images were captured on a Nikon 90i microscope with a 40×, 0.95 NA Plan Apo objective. GFP was viewed with a Brightline-Semrock FITC filter set (FITC-2024C; excitation 482 nm, emission 536 nm, dichroic 506 nm), Alexa-Fluor 568 was viewed with a Brightline-Semrock TRITC filter set (TRITC-B; excitation 543 nm, emission 593 nm, dichroic 562 nm), each mounted in Nikon TE2000 cubes. Digital images (1280 × 960 pixels) were acquired with Nikon's NIS Elements software, saved as JPEG files and minimally processed for dynamic range, then sharpened using the unsharpen mask feature (60%, 2 pixel radius) in Adobe Photoshop.

Statistics

Prism (GraphPad Software, San Diego, CA, USA) software was used to perform statistical tests. Student's paired *t* test was used to compare transfected cells *vs.* their same slice controls throughout and summary data are presented as means ± SD, unless noted otherwise. We used a one-way ANOVA to compare all four experimental groups, with post-hoc Tukey's multiple comparisons tests to determine which individual means differed. *P* values of <0.05 were considered to be significantly different. Sample population data are represented as scatterplots, bar charts of mean ± SD or as box plots (Tukey, 1977). Box plots indicate the upper and lower quartiles as edges of the box, with the median represented as a line crossing the box. The stems indicate the largest and smallest non-outlying values. Outliers are indicated with an asterisk. Outlying values are >1.5 times the quartile boundaries and extreme outlying values are >3.0 times the quartile boundaries.

Results

We recorded from visually identified pyramidal neurons using IR-DIC optics and whole cell patch clamp in current or voltage clamp. Since we could not control *a priori* which cells were transfected by the bullets, we recorded from pyramidal cells in either layers 2, 3 or 5 of rat somatosensory or motor cortex (combined: sensorimotor cortex) in organotypic slice cultures (Fig. 1*A*). About 70% of the cells sampled during the present study were from primary somatosensory cortex and 30% from motor cortex. There are differences in pyramidal cell physiology between these two areas with the main example being that some pyramidal cells in layer 5B of motor cortex accelerate during repetitive firing, a pattern not observed in somatosensory cortex (Miller *et al.* 2008). We did not encounter accelerating layer 5B cells in the present study and, regardless, we matched transfected cells with untransfected cells from the same cortical area and layer. Cells included for further analysis had an RMP more negative than –65 mV and overshooting APs.

Transfected cells had to fulfil three criteria: the cell had to be GFP-positive (green), contain a visible gold bullet (Fig. 1*B*) and respond to positive or negative pressure after completion of the recording (to ensure that we recorded

from the green cell rather than an adjacent one). In these experiments, we paired a recording of a transfected (green) cell with a recording of an untransfected cell (control) from the same slice, cortical area and cortical layer (within ~50 μm). In most cases the cell pairs were recorded sequentially, although in a few cases they were recorded simultaneously as dual recordings. In other experiments, we transfected cells with cDNA for GFP alone or with

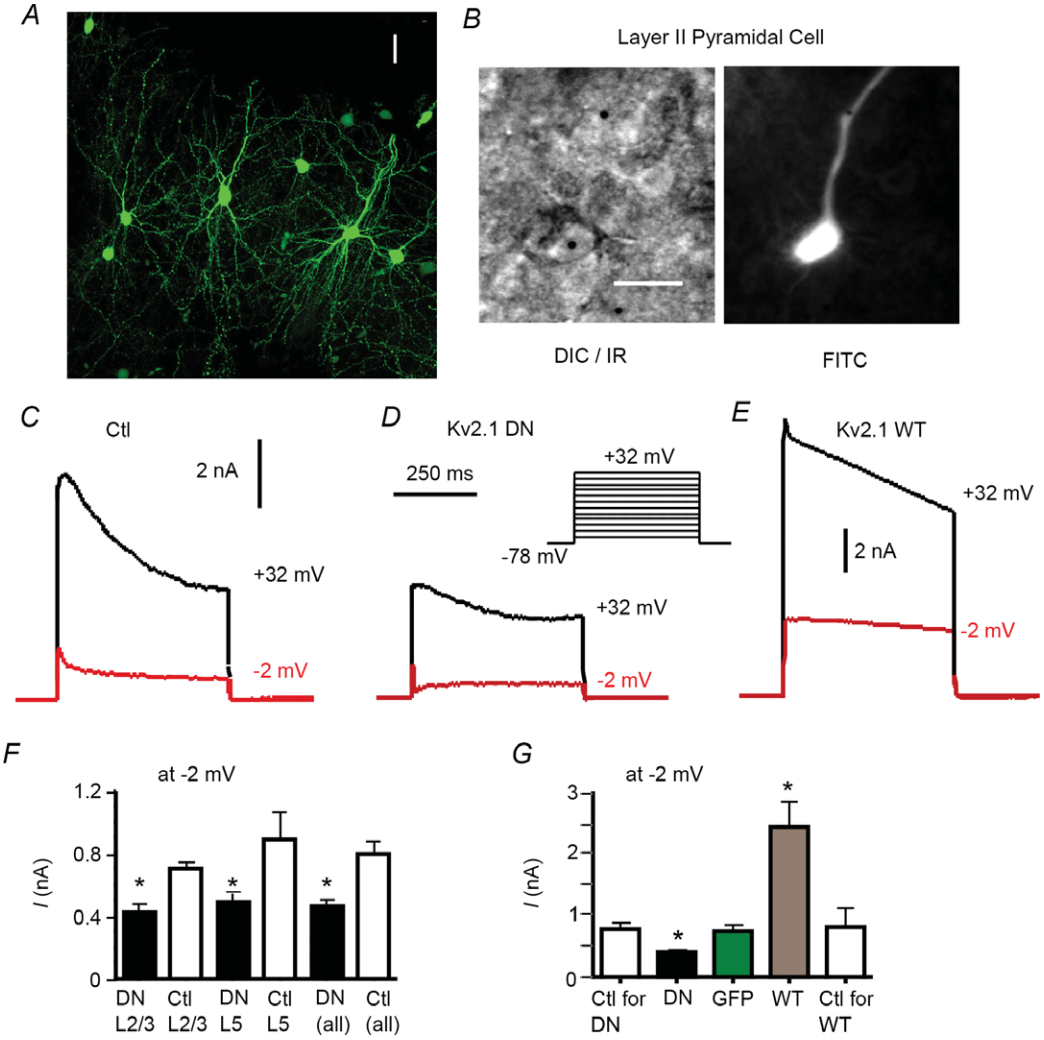

Figure 1. Biolistic transfection and voltage clamp data
Biolistic (gene gun) transfection with cDNA for wild-type (Kv2.1 WT) or pore mutant Kv2.1 (Kv2.1 DN) altered whole cell outward currents in neocortical pyramidal neurons. *A*, confocal projection from Z-stack illustrating GFP expression in pyramidal and non-pyramidal neurons in layer 2/3 of rat somatosensory cortex in organotypic slice culture. Cells were transfected with cDNA for GFP and a non-conducting Kv2.1 pore mutant that acts as a dominant negative (Kv2.1 DN). Scale bar = 25 μm. *B*, *left:* IR/DIC image of transfected layer 2/3 pyramidal cell. Note gold 'bullet' (black circle) in cell. Scale bar = 25 μm. *Right:* FITC fluorescent image of the same cell, showing GFP expression. *C*, whole cell voltage clamp records from a non-transfected control cell. A family of voltage steps were made in 10 mV increments, nominally between –68 and +32 mV (see inset in *D*). Traces are shown for steps to +32 mV (black) and –2 mV (red). *D*, similar traces from a cell transfected with GFP and the Kv2.1 DN construct. Note smaller current amplitude and more obvious A-type current at –10 mV. *E*, traces for a cell transfected with GFP plus the Kv2.1 WT cDNA (Kv2.1 overexpression). Note the greatly enhanced current amplitude. *F*, bar chart showing mean amplitude (at 200 ms after step initiation) for non-transfected control (Ctl) *vs.* dominant negative (Kv2.1 DN) groups for pyramidal cells in layer 2/3 (L2/3), layer 5 (L5) and combined layers 2/3 and 5 (all). There were no significant differences between the various non-transfected (Ctl) groups. For all layers, the Kv2.1 DN cells had lower current amplitudes than matched non-transfected (Ctl) cells. *G*, for all layers combined, there was a significant reduction in current amplitude (at –2 mV) in the Kv2.1 DN group *vs.* the non-transfected group. There was no difference between non-transfected cells and cells transfected with GFP alone. Current amplitude was significantly increased in cells overexpressing the Kv2.1 WT cDNA (GFP non-transfected control group not shown).

cDNA for GFP plus WT Kv2.1 (also a gift from Drs Jeanne Nerbonne and James Trimmer). Since there is extensive overlap in the distribution and expression of Kv2.1 and Kv2.2 subunits in neocortical pyramidal and other neurons (Kihira *et al.* 2010, Hermanstyne *et al.* 2010) and we cannot determine whether Kv2.2-mediated currents are also altered by our treatments, we refer to changes in Kv2-mediated currents and functions.

Voltage clamp

We first used whole cell recordings in voltage-clamp mode to assess whether our manipulations altered the functional expression of Kv2 channels. Space clamp is compromised in these recordings from dendritic neurons but our goal was to compare relative amplitudes and not to determine detailed kinetics or voltage dependence. Accordingly, we also did not routinely employ series resistance or whole cell capacitance compensation for these recordings. We only accepted stable recordings with <20 MΩ series resistance (series resistance was 8–10 MΩ on average and did not differ between experimental groups). We tested K^+ currents with 0.5–1 μM TTX in the bath (to block voltage-gated Na^+ channels) and 10 mM BAPTA in the internal recording solution (to prevent activation of Ca^{2+}-dependent K^+ currents). We elicited a family of currents in response to 500 ms or 1 s voltage steps from a holding potential (HP) of –78 mV to various test potentials ranging from –68 to +32 mV (Fig. 1*C*–*E*).

Outward K^+ current (measured at 200 ms after stimulus onset to minimize contribution of the transient, A-type current) was significantly reduced in Kv2.1 DN *vs.* matched non-transfected cells (Fig. 1*C vs. D*). Similar findings were obtained when comparing the response to the largest step (nominally +32 mV) or at –2 mV (a potential used in our previous work to compare various Kv currents in these cells: Guan *et al.* 2006, 2007*a*,*b*, 2011*a*,*b*; Table 1). On average, current in Kv2.1 DN cells was 55% that of control cells (438 pA *vs.* 793 pA at –10 mV; $n = 30$ cells of each type). The Kv2.1 DN cells had a more easily observed A-type current (Fig. 1*D*), with obvious kinetic separation from the remaining very slowly activating current. We obtained similar effects of the Kv2.1 DN in layers 2/3 pyramidal cells ($n = 15$ pairs) and layer 5 cells ($n = 15$ pairs) compared to their respective paired non-transfected cells (Fig. 1*F*). Therefore, data from layers 2/3 and layer 5 cells (and their respective non-transfected cells) were combined for subsequent comparisons. There were no significant differences between the various non-transfected control groups (Fig. 1*F*).

Currents from cells transfected with GFP alone did not differ in amplitude from untransfected controls (Fig. 1*G*). In contrast, cells transfected with WT Kv2.1 had greatly increased outward currents (~300%: Table 1, Fig. 1*E* and *G*). Collectively, these data suggest that biolistic transfection was able to effectively manipulate the expression of a component of the delayed rectifier K^+ current whose properties are consistent with Kv2-mediated current (Guan *et al.* 2007*b*) and that any compensatory changes in other Kv channels must be insufficient to restore the full current amplitude.

Table 1. Voltage-clamp data

	I (pA): + 40 mV	*I* (pA): −10 mV
NT	3430 ± 186(30)	793 ± 92(30)
GFP alone	3019 ± 225(8)	800 ± 116(9)
GFP control (NT)	3312 ± 456(8)	763 ± 57(8)
Kv2.1 DN	2177 ± 173(30)*	438 ± 35(30)*
Kv2.1WT	11000 ± 1268(11)*	2420 ± 435(11)*
WT control (NT)	2778 ± 270(11)	847 ± 308(11)

All measurements were made at 200 ms after the beginning of the voltage step. Holding potential was –78 mV. Data are presented as mean ± SEM (number of cells). Transfected cells were paired with a non-transfected control cell selected in the same layer in the same slice, within ~50 μm. NT = non-transfected control cells for Kv2.1 DN experiments. Kv2.1 DN = Kv2.1 pore mutant dominant negative construct. GFP control (NT) = non-transfected cells paired with GFP alone cells. Kv2.1 WT = wild-type Kv2.1 (overexpression). WT control (NT) = non-transfected cells paired with Kv2.1 WT overexpression group. *Significant difference from control ($P < 0.05$).

Immunocytochemistry

As a further qualitative control for expression, immunocytochemistry was performed on four slices that contained cells transfected with the Kv2.1 DN and four slices containing cells overexpressing Kv2.1 WT. The staining pattern for transfected cells was compared to untransfected cells in the same slice. We used a monoclonal antibody to the C terminus of Kv2.1 (K89/34: Murakoshi & Trimmer, 1999) that was obtained from Neuromab (UC Davis). The GFP-positive cell in Fig. 2*A* and *D* was transfected with the Kv2.1 DN and GFP. There were no gross abnormalities in the distribution of Kv2.1 subunits in this cell. Figure 2*D* shows the typical clustered distribution of Kv2.1 subunits on the soma and proximal dendrites of the transfected and non-transfected pyramidal cells (cf. Murakoshi & Trimmer, 1999; Guan *et al.* 2007*b*). We found variability in the staining intensity and pattern for transfected cells. While some Kv2.1 DN cells exhibited the normal clustered pattern of Kv2.1 expression (e.g. cell marked with an arrow in Fig. 2*A*, *D* and cell marked with double arrows in Fig. 2*B*, *E*), other Kv2.1 DN cells (cell marked with a single arrow in Fig. 2*E*) and most cells with overexpression of Kv2.1 WT had increased staining

with an apparently more uniform distribution. The Kv2.1 WT cells shown in Fig. 2*C* and *F* showed intense staining relative to non-transfected cells but the clustered pattern was retained.

Functional consequences

We previously showed that in acutely dissociated pyramidal cells, Kv2-mediated currents activate more slowly than Kv1- or Kv4-mediated currents but more rapidly than Kv7-mediated currents (Guan *et al.* 2006, 2007*a*,*b*, 2011*a*,*b*). Furthermore, Kv2-mediated currents have a relatively depolarized activation range (depolarized to –40 mV: suprathreshold for APs; Guan *et al.* 2007*b*). Here we used current-clamp recordings to assess the functional consequences of manipulating Kv2 expression.

Consistent with the slow activation kinetics and depolarized activation range of Kv2 currents (Guan *et al.* 2007*b*), we found no significant differences in RMP or input resistance (R_{in}: Fig. 3*B*, Table 2). Rheobase (the current at which an AP can first be obtained in response to long current steps: Fig. 3*C*) was also not significantly different between Kv2.1 DN (218 ± 35 pA) and non-transfected cells (171 ± 18 pA: $n = 12$ pairs of cells). We also found no significant differences for any measured parameters of single APs (in response to 10–20 ms, just suprathreshold current injections) between any of the experimental groups *vs.* their paired non-transfected cells (Fig. 3*A*, Table 2). Together these data suggest minimal involvement of Kv2 channels in determining passive or single AP properties in neocortical pyramidal neurons.

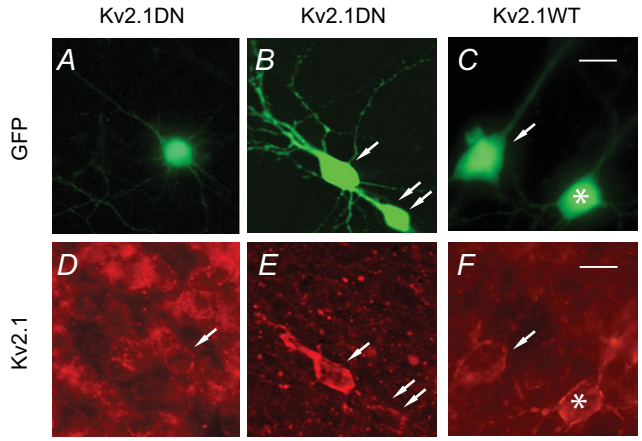

Figure 2. Immunocytochemistry
We stained organotypic slices with the Neuromab Kv2.1 monoclonal antibody (K89/34). Slices contained non-transfected cells and cells with GFP fluorescence, indicating biolistic transfection with GFP plus the Kv2.1 DN construct (*A*, *D* and *B*, *E*), or GFP plus overexpression of Kv2.1 WT (*C*, *F*). Note the differing exposures in *D vs. E* and *F*. In *E* and *F* we focused on the enhanced, brighter staining of the transfected cells at the expense of viewing non-transfected cells, and thus the background is dimmer. Non-transfected cells (no GFP fluorescence) showed a typical patchy distribution of clusters of channels on the soma and proximal apical dendrites (*D*). The staining pattern was similar for some cells expressing the Kv2.1 DN (e.g. cell with arrow in *D*, cell marked with double arrow in *E*). Other cells transfected with the Kv2.1 DN (cell marked with single arrow in *E*) and most cells transfected with the Kv2.1 WT appeared more intensely stained with a more continuous pattern. The Kv2.1 WT cells in *F* (arrow, asterisk) showed intense staining compared to non-transfected cells but retained a clustered distribution. Scale bars = 25 μm.

Repetitive firing

Based upon their slow kinetics of deactivation and inactivation (Guan *et al.* 2007*b*), we hypothesized that Kv2 channels would regulate ISIs and repetitive firing in neocortical pyramidal neurons (cf. Du *et al.* 2000; Malin and Nerbonne, 2002; Johnston *et al.* 2008). Consistent with this hypothesis, we observed that otherwise healthy Kv2.1 DN cells were less likely to fire repetitively. We tested 12 pairs of Kv2.1 DN and non-transfected cells that fired repetitively for at least 200 ms. Whereas 11 of 12 control cells fired throughout 500 ms current injections, only 6/12 Kv2.1 DN cells did so (*vs.* 4 of 6 for cells transfected with GFP alone or 6 of 8 of the Kv2.1 WT overexpression cells). In the Kv2.1 DN cells, spike amplitudes declined and the cells eventually failed to spike after 250–300 ms. Such failures to fire occurred at significantly lower stimulus intensity levels in Kv2.1 DN cells (2.9 ± 0.8 times rheobase) *vs.* paired control cells (7.25 ± 1.8 times rheobase: $P < 0.03$).

We compared firing over the initial 200 ms for these same 12 pairs of Kv2.1 DN and non-transfected cells (all layers combined) and found that Kv2.1 DN cells fired more slowly to a given input than non-transfected cells (Fig. 4). In addition, the slope of average firing frequency *vs.* injected current (*f–I* curve) was significantly less steep (lower gain) in the Kv2.1 DN cells (46 ± 8 *vs.* 103 ± 18 Hz nA^{-1}, respectively), such that the differences between non-transfected and Kv2.1 DN groups were greater for larger current injections and higher firing rates (Fig. 4*C*, *F*). The *f–I* slope for cells transfected with GFP alone (128 ± 7.1 Hz nA^{-1}; $n = 11$ cells) or Kv2.1 WT (77 ± 3.3; $n = 14$ cells) did not differ significantly from non-transfected cells.

To facilitate comparisons between cells, we plotted firing rates as a function of multiples of rheobase (Fig. 4*G–I*). Under these conditions, firing rates and gain remained significantly lower for the Kv2.1 DN group *vs.* paired non-transfected cells. The differences between non-transfected and Kv2.1 DN groups were greater for larger current injections and higher firing rates. The *f–I* slope was significantly less steep (lower gain) in the Kv2.1 DN group [19.9 ± 2.5 Hz (multiple of rheobase)$^{-1}$] *vs.* non-transfected cells [32.5 ± 3.5 Hz

(multiple of rheobase)$^{-1}$; $P = 0.007$; Fig. 4*I*], resulting in significant differences in firing rate at 3× rheobase. Similar results were obtained for layer 2/3 pyramidal cells ($n = 7$ pairs; non-transfected: 34.0 ± 5.9 Hz rheobase^{-1} *vs.* Kv2.1 DN: 21.2 ± 2.8 Hz rheobase^{-1}; $P < 0.03$) and for layer 5 pyramidal cells ($n = 5$ pairs; non-transfected: 30.4 ± 1.8 Hz rheobase^{-1} *vs.* Kv2.1 DN: 18.1 ± 4.9 Hz rheobase^{-1}; $P < 0.046$: Fig. 4*I*). Finally, we also tested a subset of eight pairs of pyramidal neurons over a longer, 500 ms, epoch of repetitive firing. Again the Kv2.1 DN group fired significantly slower and with lower gain than paired non-transfected cells (15.9 ± 2.29 *vs.* 29.0 ± 4.45 Hz rheobase^{-1}; $P < 0.01$).

Cells transfected with GFP alone did not differ in firing rate from their paired non-transfected cells. For 200 ms firing, the non-transfected cells fired with a slope of 32.9 ± 3.3 Hz rheobase^{-1}, similar to paired cells transfected with GFP alone (33.1 ± 8.3 Hz rheobase^{-1}; $n = 7$ cells). Eight pairs were tested (200 ms firing) to compare overexpression of Kv2.1 WT (22.2 ± 7.3 Hz rheobase^{-1}) *vs.* matched non-transfected cells (27.2 ± 5.3 Hz rheobase^{-1}), with no statistical differences observed between the groups.

Spike frequency adaptation

The Kv2.1 DN group also differed from their paired non-transfected cells in the relationship between instantaneous firing frequency (1/ISI) and time (*f–t* plot: Fig. 5). Figure 5*A* shows typical firing during the initial 100 ms in response to a 500 ms current injection at 3× rheobase (Fig. 5*Aa*) as well as later in the firing epoch (240–340 ms: Fig. 5*Ab*). Firing of the non-transfected cell is shown in black and the paired Kv2.1 DN cell in red. In both groups, firing rate is initially high but declines with time (SFA). While firing appears to be very similar for non-transfected and Kv2.1 DN cells during the first ∼50 ms of firing, spikes progressively fall relatively later in time for the Kv2.1 DN cells as the stimulus is continued. Note also the more depolarized ISI, greater increase in spike threshold and greater decline in spike height for the Kv2.1 DN trace. Comparison of the average *f–t* relationship for 11 pairs (6 from layer 2/3; 5 from layer 5) of Kv2.1 DN and non-transfected cells revealed more pronounced SFA in the Kv2.1 DN cells (at 3× rheobase: Fig. 5*B*). Percentage adaptation (instantaneous frequency at AP no. 10/initial firing frequency) was significantly greater in Kv2.1 DN cells ($57 \pm 4.7\%$) than in non-transfected cells ($42 \pm 3.9\%$: ISIs normalized to the 2nd ISI; one-way ANOVA with post-hoc multiple comparisons test). Percentage adaptation did not differ between non-transfected cells and cells transfected with GFP alone ($36 \pm 6.5\%$, $n = 11$) or with overexpressed Kv2.1 WT ($32 \pm 3.8\%$, $n = 11$: Fig. 5*B*). Could this increased SFA be the mechanism underlying the reduced gain and firing rates in Kv2.1 DN cells?

Possible mechanisms for changes in repetitive firing

We hypothesized that Kv2 channels may exert effects on firing rate by regulating the membrane potentials attained during ISIs and thereby affecting inactivation of voltage-gated Na^+ channels responsible for the AP upstroke (Johnston *et al.* 2008).

As with isolated APs (see above), we found no differences between experimental groups in the properties of the first AP during repetitive firing in response to a 3× rheobase current injection (Table 3). In Fig. 5, we plotted values for several spike parameters for successive APs during repetitive firing elicited by

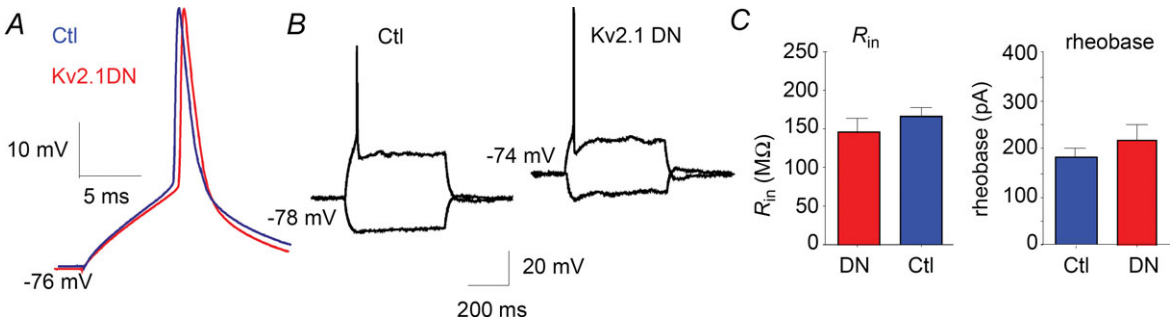

Figure 3. Passive properties and single AP properties
Transfection with the Kv2.1 DN did not lead to changes in passive properties or properties of single APs. *A*, superimposed representative APs from a non-transfected (Ctl) layer 2/3 pyramidal cell and Kv2.1 DN cell from the same slice and layer. We found no differences between Kv2.1 DN and non-transfected control groups for any measured parameters of single APs (amplitude, threshold, d*V*/d*t*, half-width: APs elicited with suprathreshold 10 ms current injection). *B*, traces from a different pair of non-transfected cell (left) and Kv2.1 DN cell (right) indicate no changes in input resistance in the Kv2.1 DN cells. *C*, *left:* bar chart indicating no significant differences for input resistance between Kv2.1 DN and non-transfected (Ctl) cells. *Right:* rheobase did not differ in the Kv2.1 DN group *vs.* non-transfected (Ctl: $n = 12$ pairs of cells).

Table 2. Passive properties and single action potentials (10–20 ms current injection)

	RMP (mV)	R_{in} (MΩ)	AP (mV)	V_{th} (mV)	AP HW (ms)	dV/dt up (V s^{-1})	dV/dt down (V s^{-1})
NT	−70 ± 2 (23)	145 ± 10 (23)	90 ± 2 (23)	−44 ± 0.8 (23)	1.74 ± 0.1 (23)	211 ± 14 (23)	54 ± 6 (23)
Kv2.1 DN	−71 ± 2 (23)	166 ± 17 (23)	91 ± 2 (23)	−43 ± 1.0 (23)	1.76 ± 0.1 (23)	213 ± 15 (23)	53 ± 5 (23)
GFP NT	−67 ± 2.2 (17)	130 ± 14 (17)	92 ± 2 (17)	−43 ± 0.8 (17)	1.56 ± 0.2 (17)	251 ± 18 (17)	54 ± 4 (17)
GFP alone	−70 ± 2.2 (17)	154 ± 22 (17)	92 ± 2 (17)	−43 ± 0.8 (17)	1.54 ± 0.1 (17)	243 ± 21 (17)	55 ± 4 (17)
Kv2.1 WT NT	−69 ± 1.8 (6)	162 ± 27 (6)	95 ± 1.6 (6)	−45 ± 1.4 (6)	1.73 ± 0.15 (6)	228 ± 14 (6)	50 ± 10 (6)
Kv2.1 WT	−67 ± 1.3 (6)	199 ± 42 (6)	88 ± 6 (6)	−42 ± 1.2 (6)	1.53 ± 0.1 (6)	175 ± 31 (6)	54 ± 6 (6)

There were no significant statistical differences between groups. Data are presented as mean ± SEM (number of cells). Non-transfected cells were paired with experimental treatments by selecting a non-transfected cell in the same layer in the same slice (within ∼50 μm). Kv2.1 DN = Kv2.1 pore mutant dominant negative construct. GFP = transfected with DNA for GFP only. GFP NT = paired non-transfected cells for GFP alone group. Kv2.1 WT = wild-type Kv2.1 (overexpression). Kv2.1 WT NT = non-transfected cells paired with WT overexpression group. RMP = resting membrane potential. R_{in} = input resistance. AP = action potential. V_{th} = voltage threshold for AP. HW = half width of AP (see Methods). dV/dt = maximum of first derivative of voltage for AP upstroke (up) or repolarization (down). [1] dV/dt of AP are reported in V/s.

a long DC current injection. In non-transfected cells, these spike parameters gradually change with successive spikes and approached a plateau for a given current injection (Fig. 5*C*–*F*). The plateau levels (measured at AP no. 10) differed significantly from initial values (AP no. 1) within all experimental groups (non-transfected, Kv2.1 DN, GFP alone, Kv2.1 WT) for AP voltage threshold, minimum voltage during the ISI, dV/dt for spike up- and down-stroke, and AP half-width (HW) (Fig. 5, Table 3). All of these changes appeared more pronounced in the Kv2.1 DN cells than in paired non-transfected cells, although for most parameters the differences did not reach statistical significance. A similar pattern was evident for AP amplitude (e.g. for non-transfected cells AP1 = 90 ± 2.6 mV and AP10 = 85 ± 2.3 mV; for the Kv2.1 DN cells AP1 = 94 ± 2.5 mV and AP10 = 85 ± 3.2 mV; n = 10 cells in each group) and AP HW (for non-transfected cells HW1 = 1.4 ± 0.3 mV and HW10 = 2.7 ± 0.6 mV; for the Kv2.1 DN cells HW1 = 1.4 ± 0.2 mV and HW10 = 5.8 ± 2.6 mV; n = 10 cells in each group). No significant differences from non-transfected controls were observed for the changes in any of the parameters with transfection of GFP alone or with overexpression of Kv2.1 WT (Fig. 5, Table 3). Interestingly, for most parameters there was a trend for Kv2.1 WT cells to differ from non-transfected cells in the opposite direction from Kv2.1 DN cells, resulting in the greatest differences being between the Kv2.1 DN and Kv2.1 WT groups. The only significant differences between experimental groups were for the change in dV/dt for both the rise and the fall of the AP (normalized to the first AP). In a paired t test between Kv2.1 DN and paired non-transfected cells, the change from the first to tenth spike was significantly different for the spike upstroke dV/dt ($P < 0.04$) and for spike downstroke dV/dt ($P < 0.04$). An ANOVA between all experimental groups was also significant for both of these parameters ($P < 0.025$ for dV/dt for the upstroke; $P < 0.0079$ for dV/dt for repolarization). The only means found to differ significantly in a *post hoc* Tukey's multiple comparisons test were the Kv2.1 DN *vs.* Kv2.1 WT groups (dV/dt for both upstroke and repolarization).

Our data suggest that reduction of Kv2 expression (Kv2.1 DN cells) resulted in a trend to progressively more depolarized ISIs with successive APs during a spike train (see traces in Fig. 5*A*), but the minimum voltages attained during the ISI (−43.7 ± 2.4 mV for the 8th–10th APs) were not significantly different between Kv2.1 DN cells and matched non-transfected cells (−45 ± 2.1 mV; $P < 0.23$; Fig. 5*C*–*F*). Plots of dV/dt *vs.* V (phase plots) revealed qualitatively greater changes in dV/dt *vs.* V_m trajectories during the spike train in Kv2.1 DN cells, as can be seen in Fig. 6*A* and *B* (in response to 3× rheobase current injection). In both non-transfected and Kv2.1 DN cells there was a large change in the trajectory of the phase plot between the first and second AP. In non-transfected cells the subsequent spikes were similar, resulting in a gradual constriction of the trajectories. In contrast, this change was more dramatic in Kv2.1 DN cells, reflecting greater changes in both AP amplitude and especially dV/dt (upstroke and downstroke). Similar results were obtained for 11 of 12 pairs of Kv2.1 DN and non-transfected cells.

We hypothesized that reduced availability of Na^+ channels was responsible for the reduced dV/dt for the AP upstroke. Henze and Buzsaki (2001) reported that threshold and spike rate of rise in hippocampal neurons varied as a function of the preceeding ISI. It is difficult to directly test this hypothesis using voltage clamp in these dendritic neurons, although the maximum dV/dt of the spike upstroke is highly correlated with Na^+ channel activation and is widely considered an excellent surrogate to voltage clamp data as an index of Na^+ channel availability (e.g. Madeja, 2000; Higgs *et al.* 2006; Bean, 2007; Johnston *et al.* 2008; Higgs & Spain, 2011). In

all experimental and control groups we found a strong correlation between the minimum potential during a given ISI with properties of the subsequent spike. For example, in control cells maximal dV/dt was highly correlated with the minimal potential during the previous ISI (e.g. $r = -0.76$ for the ninth ISI, 3× rheobase stimulus). This correlation is also present in the Kv2.1 DN group ($r = -0.79$ for the ninth ISI, 3× rheobase stimulus). Although we did not observe a significant difference in the change in minimum voltage during the ISI between non-transfected and Kv2.1 DN cells (Fig. 5*C*), cells transfected with the Kv2.1 DN did show a significantly greater decrease in dV/dt (upstroke and repolarization) with successive APs during a spike train (Figs 5*E*, *F* and 6).

Mechanisms for increased SFA in DN cells

In cortical pyramidal cells, the slow afterhyperpolarization (sAHP) conductance is a primary mechanism controlling

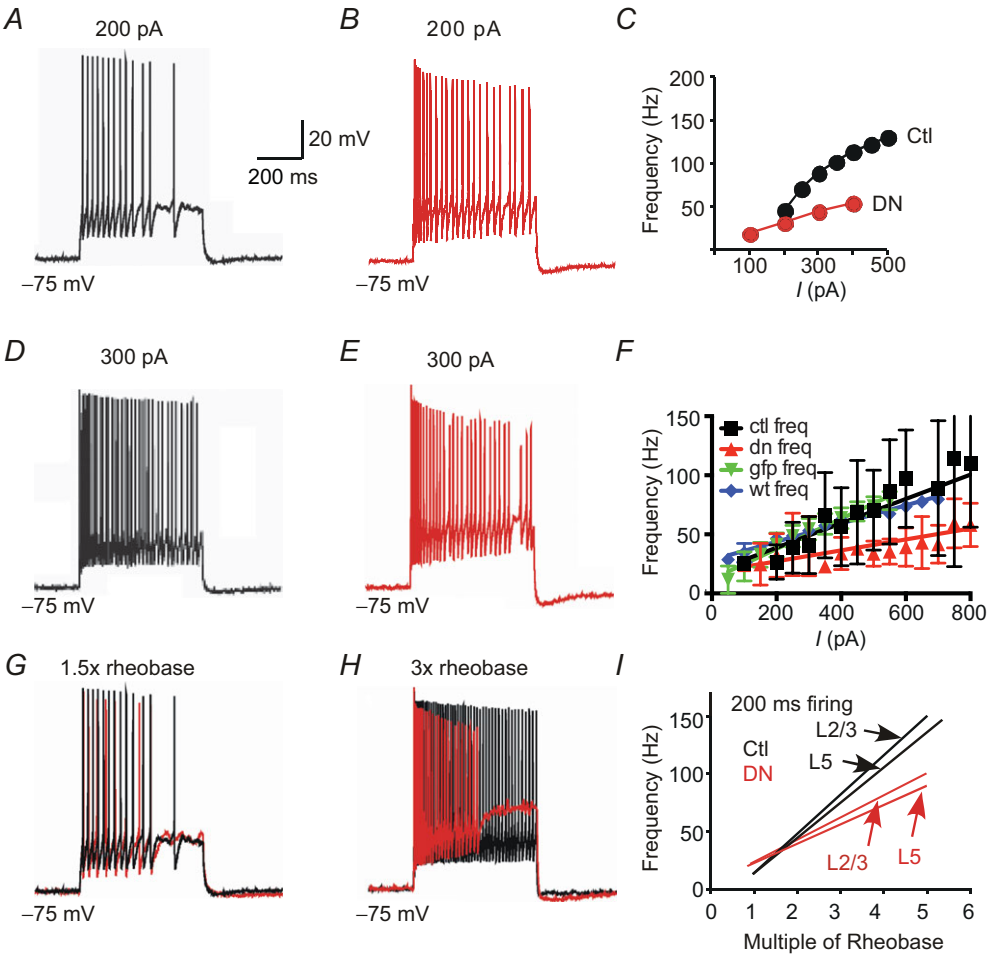

Figure 4. Repetitive firing
A, voltage trace in response to 200 pA current injection (500 ms) in a non-transfected layer 5 pyramidal cell. *B*, response of Kv2.1 DN transfected cell in same slice and layer as *A* (200 pA step current injection). *C*, plot of average firing frequency *vs.* injected current (*I*) for the cells shown in *A* and *B*. Note faster firing and steeper *f–I* slope in non-transfected (Ctl) cells (black circles) *vs.* Kv2.1 DN (red circles). *D*, response of same cell as in *A* to a larger (300 pA) current injection. Note faster firing *vs.* *A*. *E*, response of same Kv2.1 DN cell as in *B* to 300 pA current injection. Note faster initial firing *vs.* *B*, followed by a decline in spike height and eventual spike failure. *F*, plot of average firing frequency *vs.* injected current (*I*) for 12 pairs of non-transfected (Ctl) and Kv2.1 DN cells, as well as GFP alone ($n = 7$ cells) and Kv2.1 WT ($n = 8$ cells). Note lower slope (gain) and slower firing in the Kv2.1 DN cells (red). *G*, response of same cells as in *A* and *B* to a current injection at 1.5× rheobase. The non-transfected trace is black and Kv2.1 DN trace is red (there was little difference between the cells at this current). *H*, response of same cells in *A* and *B* to a larger current injection (3× rheobase). Same colour scheme as in *G*. Note depolarized V_m during ISIs and spike failure in the Kv2.1 N cell. *I*, plot of average firing frequency *vs.* multiple of rheobase. We compared non-transfected *vs.* Kv2.1 DN cells separately for layers 2/3 and for layer 5. In each case, the Kv2.1 DN cells fire slower and gain is lower. Individual data points are not included for clarity.

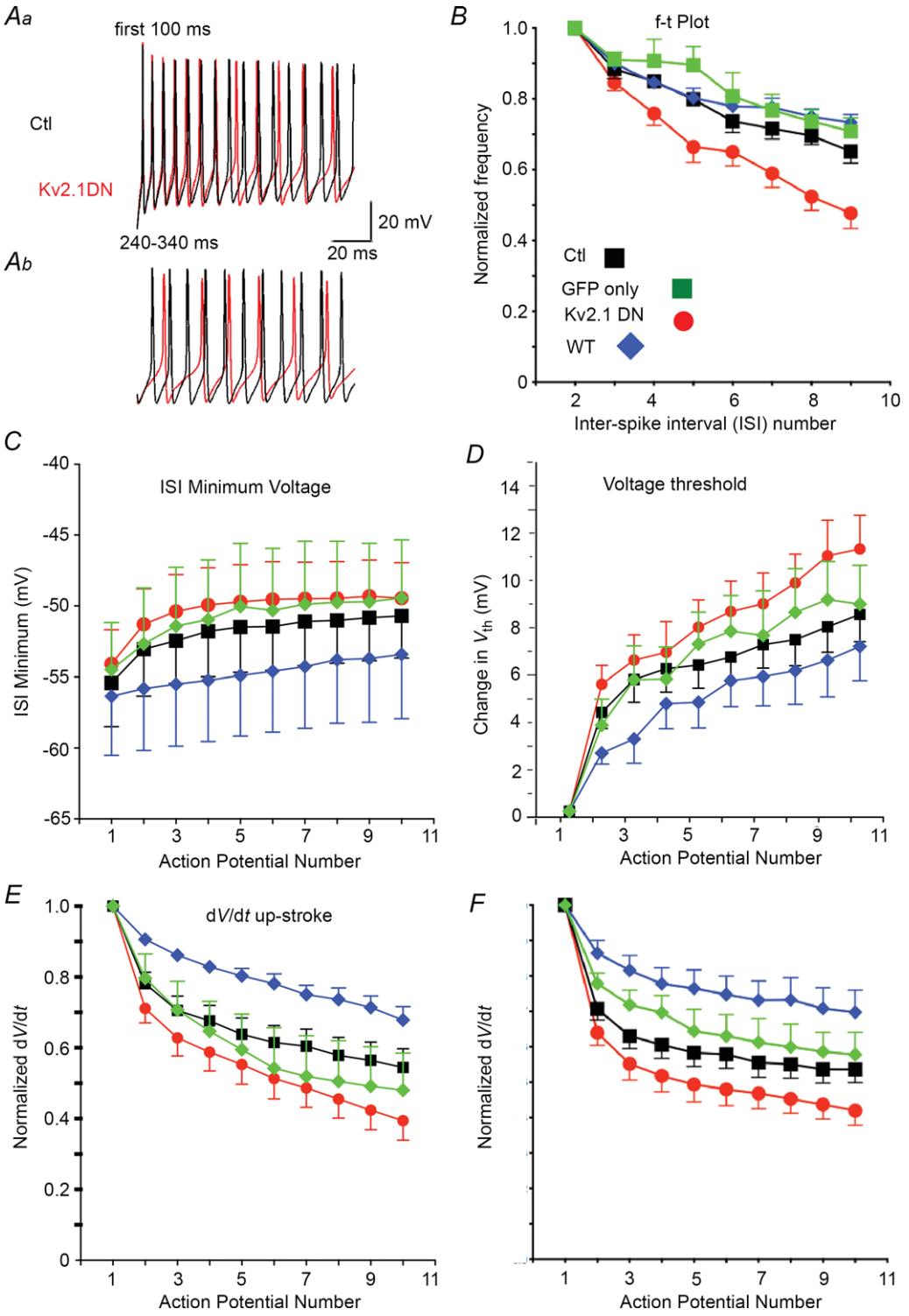

Figure 5. Spike frequency adaptation
A, repetitive firing from the same cells as in Fig. 4*A* and *B* for the time epochs indicated. Non-transfected (Ctl) trace is black and Kv2.1 DN trace is red. *Aa*, Firing is similar initially. The Kv2.1 DN trace becomes more depolarized during ISIs and firing slows towards the end of the first 100 ms of firing. *Ab*, firing in the same cells at 240–340 ms after initial current injection. Note the depolarized ISI and voltage threshold, slowed firing, and reduced spike amplitude in the Kv2.1 DN cell. *B*, plots for instantaneous firing frequency (1/ISI) normalized to the second ISI and as a function of ISI number. Experimental groups are indicated by colour (inset in *E*). Non-transfected (Ctl) cells are shown in black, cells transfected with GFP alone in green, Kv2.1 DN cells in red and cells with overexpressed Kv2.1 WT in blue. While GFP alone or Kv2.1 WT caused no significant change in this relationship, the Kv2.1 DN

SFA (Madison & Nicoll, 1984; Schwindt *et al.* 1988). Thus, a possible mechanism for the increase in SFA observed in the Kv2.1 DN cells would be an increase in the conductance underlying the sAHP. We found that the sAHP (measured 500 ms after the peak AHP following spiking to minimize contribution of SK channels: Schwindt *et al.* 1988; Abel *et al.* 2004) was not significantly larger (6.4 ± 0.3 *vs.* 4.95 ± 0.8 mV) following repetitive firing in response to a 500 ms DC current injection at a given current injection in Kv2.1 DN cells *vs.* paired non-transfected cells, although there were fewer APs in the Kv2.1 DN cells (data not shown).

Since the sAHP is sensitive to the number and frequency of APs (Abel *et al.* 2004), which differed between non-transfected and Kv2.1 DN groups, we also compared cells with a protocol where we delivered 10, 5 ms suprathreshold current injections at 50 Hz (Fig. 7). Again, we found no differences between Kv2.1 DN (2.4 ± 0.6 mV, $n = 16$) and non-transfected cells (2.1 ± 0.4 mV, $n = 32$) for the sAHP (measured at 500 ms) or the peak AHP (DN: 4.1 ± 0.6 mV, $n = 19$; Control: 4.0 ± 0.4 mV; $n = 28$; Fig. 7*A*, *B*). The sAHP in cells expressing GFP alone (1.7 ± 0.6 mV; $n = 15$) and Kv2.1 WT-overexpressing cells (0.9 ± 0.6 mV; $n = 12$) also did not differ from non-transfected cells. For the peak AHP the values were also not different (GFP: 3.5 ± 0.4 mV, $n = 15$; Kv2.1 WT: 3.4 ± 0.4, $n = 14$).

When we compared the first *vs.* tenth AP elicited by repeated brief current injections at 50 Hz, we found no differences in spike parameters between any of the experimental groups (Fig. 7*E*–*G*). This included dV/dt measurements, which were significantly different between non-transfected and Kv2.1 DN groups during repetitive firing. Similarly, phase plots for the 10 APs elicited at 50 Hz did not differ between non-transfected and Kv2.1 DN cells (Fig. 6*C*, *D*). The main difference between these two different protocols for eliciting spike trains is the lack of sustained depolarization between spikes for the 10 AP at 50 Hz protocol (Figs 6*C*, *D* and 7*C*, *D*). Collectively, these data suggest that the increased SFA with prolonged DC current injections (cf. Fig. 5) was not due to a compensatory increase in the sAHP (although the sustained depolarization during repetitive firing to DC current could result in increased Ca^{2+} entry: Du *et al.* 2000) and is consistent with differences in ISI voltages altering Na^+ channel availability during repetitive firing.

Discussion

Kv2.1 subunits have a nearly ubiquitous distribution in neurons. They are expressed in clusters on the soma and proximal apical dendrites of pyramidal neurons (Murakoshi & Trimmer, 1999; Guan *et al.* 2007*b*) as well as on the axonal initial segment (Sarmiere *et al.* 2008). Kv2.2 channels are expressed on the axonal initial segment of auditory neurons from the medial nucleus of the trapezoid body (MNTB: Johnston *et al.* 2008). The localization and biophysics of Kv2.1-containing channels are highly regulated by phosphorylation (Misonou *et al.* 2005*a*; Park *et al.* 2008) and have been implicated in cellular responses to seizures and ischaemia (Misonou *et al.* 2004, 2005*b*; Mohapatra *et al.* 2009), as well as changes underlying intrinsic plasticity (Nataraj *et al.* 2010) and cell death (Pal *et al.* 2003) in pyramidal neurons. Many of the Kv2.1 channels expressed in the membrane are apparently not activated by voltage steps (especially Kv2.1 channels located in clusters: O'Connell *et al.* 2010), and Kv2 channels have been implicated in non-conducting functions (Fox *et al.* 2013). For example, in some cell types, Kv2.1 channels are known to associate with SNARE proteins and facilitate exocytosis (e.g. Singer-Lahat *et al.* 2007). There is extensive overlap in the distribution and expression of Kv2.1 and Kv2.2 subunits in neocortical pyramidal neurons (Hermanstyne *et al.* 2010; Kihira *et al.* 2010) and we could not determine whether Kv2.2-mediated currents were also altered by our treatments, so we refer to Kv2-mediated currents and functions.

In this study, we tested for changes in neuronal behaviour after manipulation of expression levels of Kv2 channels in neocortical pyramidal cells in organotypic slice cultures. Reduction in Kv2 current did not affect neuronal passive properties or the properties of single APs. In contrast, loss of functional Kv2 channels caused a dramatic slowing of firing rates and reduced *f*–*I* gain. This

group showed a significantly greater decrease in firing frequency with increasing spike number (spike frequency adaptation: SFA). *C*, population data for the minimum voltage attained during the ISI for non-transfected and Kv2.1 DN cells as a function of spike number during firing (at 3× rheobase). The ISIs became more depolarized with successive spikes and this change was greater in Kv2.1 DN cells. *D*, spike voltage threshold became more depolarized with spike number and this effect appeared more pronounced in Kv2.1 DN cells *vs.* non-transfected control cells. *E*, the maximum rate of rise for the spike (dV/dt) decreased with spike number during firing and this effect was magnified in the Kv2.1 DN cells ($P = 0.04$). The difference between the Kv2.1 DN and Kv2.1 WT groups was significantly different (ANOVA and post-hoc Tukey's multiple comparisons test). *F*, the maximum rate of decay for the spike (dV/dt) slowed during firing and this effect was magnified in the Kv2.1 DN cells ($P = 0.04$). The difference between the Kv2.1 DN and Kv2.1 WT groups was significantly different (ANOVA and post-hoc Tukey's multiple comparisons test).

Table 3. Parameters for the first action potential (AP) during repetitive firing (500 ms current injection at 3× rheobase)

	NT ($n = 11$)	GFP ($n = 5$)	Kv2.1 DN ($n = 11$)	Kv2.1 WT ($n = 6$)
Voltage threshold (mV)	−47.7 ± 3.2	−44.3 ± 2.0	−46.1 ± 4.9	−42.9 ± 6.8
Minimum V_m during ISI (mV)	−55.4 ± 10.2	−54.5 ± 7.5	−54.1 ± 8.0	−56.4 ± 10.2
Maximum dV/dt for AP upstroke	247 ± 104	209 ± 77	258 ± 92	193 ± 46
Maximum dV/dt for AP downstroke	76 ± 40	66 ± 49	75 ± 40	60 ± 15

Data are presented as mean ± SEM (number of cells). There were no significant differences between experimental groups. Non-transfected (NT) cells were paired with the Kv2.1 DN cells by selecting a cell in the same layer in the same slice, within ∼50 μm. Kv2.1 DN = Kv2.1 pore mutant dominant negative construct. GFP = transfected with cDNA for GFP only. Kv2.1 WT = wild-type Kv2.1 (overexpression). Minimum V_m during ISI = AHP after first AP. n = number of cells.

was accompanied by increased spike frequency adaptation and a tendency for spiking to fail at lower stimulus levels (reduced dynamic range of firing in Kv2.1 DN cells). A significant reduction in the maximum dV/dt for the tenth AP during repetitive firing in response to a 3× rheobase current injection suggested that there is less Na^+ channel availability, probably due to more pronounced Na^+ inactivation during spike trains in the DN cells. There was a trend towards greater depolarization during the ISI in the Kv2.1 DN cells and we favour the hypothesis that Kv2 channels act to regulate the trajectory of the membrane potential during the ISI as the cause for changes in Na^+ channel availability during repetitive firing (as measured by maximum dV/dt), resulting in increased spike failure, increased spike frequency adaptation and reduced gain of firing in Kv2.1 DN cells.

A potential caveat in our study is that the pyramidal cells in organotypic culture are relatively immature (∼2 weeks) in terms of potassium channel development (Lorenzon & Foehring, 1993; Pineda *et al.* 1999; Guan *et al.* 2011*b*) and firing behaviour (McCormick & Prince, 1987; Lorenzon & Foehring, 1993). Our previous work showed that the relative proportions of the various Kv channels do not change during postnatal development but at 2 weeks the currents are small (Guan *et al.* 2011*b*). Nevertheless, a greater overall density of channels and changes in cell morphology could influence the functional consequences of reductions in Kv2 conductance. We assume that for cells transfected with GFP plus Kv2.1 DN or Kv2.1 WT, cells shown to express GFP also express the Kv2.1 DN or Kv2.1 WT. Variability in co-transfection or time after transfection may contribute to variability in our results.

Manipulations of Kv2.1 expression

Channels containing Kv2 subunits are considered to underlie much of the delayed rectifier current in neurons, although this has only been directly shown in a small number of neuron types to date. Murakoshi and Trimmer (1999) used intracellular application of an antibody to the C terminus of the Kv2.1 subunit to identify Kv2.1 as the major contributor to the delayed rectifier current in cultured hippocampal pyramidal neurons. This was confirmed using antisense treatment in cultured hippocampal pyramidal neurons (Du *et al.* 2000). Intracellular application of Kv2.1 antibodies also implicated Kv2.1 in the delayed rectifier of smooth muscle cells (Archer *et al.* 1998; Lu *et al.* 2002). Genetic manipulations of expression (e.g. with dominant negative expression) have also implicated Kv2.1 subunits underlying the delayed rectifier in the heart (Xu *et al.* 1999), sympathetic ganglia (Malin & Nerbonne, 2002) and cultured neocortical neurons (Pal *et al.* 2003). Dominant negative transfections were also used to link Kv2.2 subunits to delayed rectifier currents in *Xenopus* spinal neurons (Blaine & Ribera, 2001).

Over the time course of our experiments, transfection with the Kv2.1 DN effectively reduced the persistent outward current in pyramidal neurons (by 45% on average). Currents were unchanged by transfection with cDNA for GFP alone and were greatly enhanced (by ∼300%) by overexpression of WT Kv2.1. Previously, we used several methods to assess Kv2-mediated currents in acutely dissociated layer 2/3 neocortical pyramidal cells (Guan *et al.* 2007*b*). The peptide ω-stromatoxin (ScTx), a potent gating modifier of both Kv2.1 and Kv2.2 (Escoubas *et al.* 2002), reduced whole cell current by ∼58% (at –10 mV). Unfortunately, ScTx also effectively blocks Kv4 channels (responsible for much of the A current in pyramidal cells: Norris & Nerbonne, 2010) at similar doses (Escoubas *et al.* 2002), diminishing the value of this agent for functional studies. We also applied the same Kv2.1 antibody used by Murakoshi and Trimmer (1999) intracellularly to layer 2/3 neocortical pyramidal neurons (Guan *et al.* 2007*b*) and this blocked ∼33% of whole cell current within 8 min (20–50%). Combined with our previous estimates of the amplitude of putative Kv2 current from the ScTx experiments (∼60% of whole cell current), the present data suggest that the DN treatment reduced the Kv2-mediated current by about two-thirds on average (corresponding to a 45% reduction of the entire whole cell current, 60% of which is Kv2-mediated). This is similar to the block obtained by Malin and Nerbonne

(2002) in type 1 sympathetic ganglion cells and HEK cells (~50% of current). In that study, combined transfection of DN constructs for Kv2.1 and Kv2.2 blocked the entire delayed rectifier current. In cultured hippocampal pyramidal neurons, Du *et al.* (2000) chronically applied Kv2.1 antisense and found ~30% reduction in Kv2.1 protein after 5 days and ~90% reduction after 2 weeks. In that study, currents were reduced by 56%. Interestingly, Kihira *et al.* (2010) suggest that Kv2.1 and 2.2 subunits may form heteromultimeric channels in pyramidal cells. We did not assess the role of Kv2.2 subunits in this study but the decreased current in the Kv2.1 DN cells suggests ineffective functional compensation by upregulation of Kv2.2 subunits.

Function

We found that reducing Kv2 currents with the Kv2.1 DN construct did not affect passive membrane properties (resting membrane potential, input resistance), rheobase or the properties of single APs (voltage threshold, amplitude, half-width, width at threshold, dV/dt for polarization or repolarization, mAHP) in neocortical pyramidal cells. These findings are consistent with our previous finding that Kv2 channels are 'high threshold' channels (Guan *et al.* 2007*b*) and that significant Kv2 currents are not typically observed at subthreshold potentials (Guan *et al.* 2007*b*).

The absence of differences in single AP properties in the Kv2.1 DN cells is also consistent with the observation by Kang *et al.* (2000) that the putative delayed rectifier channel ($\gamma = 17$ pS) in layer 5 pyramidal cells was not activated by single APs. Du *et al.* (2000) also reported no changes in passive properties or single APs in cultured CA1 pyramidal neurons after Kv2.1 antisense treatment. Using the same DN construct and biolistic transfections as we used, Malin and Nerbonne (2002) found in HEK cells and sympathetic ganglion cells that in contrast to our findings in pyramidal neurons, Kv2.1 DN reduced current ~25% in response to using APs as the voltage stimulus and caused a slight broadening of the AP in tonic firing sympathetic ganglion cells in current-clamp. They found that the Kv2.2 DN also led to broader APs in tonic cells, depolarized RMP and reduced rheobase. Kv2 channels have also been implicated in repolarizing the slower APs found in *Xenopus* spinal neurons (Blaine & Ribera, 2001) but not in the more rapidly repolarizing APs from mammalian MNTB neurons (Johnston *et al.* 2008). It appears that Kv2 channels activate too slowly to affect repolarization of an isolated AP in neocortical pyramidal cells (where more rapidly activating Kv4 and Kv1 channels underlie AP repolarization: Carrasquillo *et al.* 2012).

Application of 10–30 mM TEA significantly slows AP repolarization and broadens APs in neocortical pyramidal cells (Schwindt *et al.* 1988; Lorenzon & Foehring, 1993; Locke and Nerbonne, 1997). Since Kv2-mediated currents are the largest voltage-gated K^+ currents in neocortical pyramidal neurons and this current component is blocked by millimolar TEA (Guan *et al.* 2007*b*), it is perhaps surprising that no significant effects were observed on AP parameters in cells expressing the Kv2.1 DN. It is unclear why TEA is more effective on single APs than the Kv2.1 DN. As with the Kv2.1 DN cells, TEA application does lead to slower firing and spike failure at lower firing rates (Locke & Nerbonne, 1997). Perhaps some of the effects of TEA are due to its acting on channels other than Kv2; for example, BK, Kv7 and Kv3 channels are all known to be TEA-sensitive (Coetzee *et al.* 1999). Another alternative is that other types of channels are upregulated and compensate for the loss of functional Kv2 channels for spike repolarization during the several days in organotypic slice culture (cf. Norris & Nerbonne, 2010), although we did not observe any clear trends for changes with time *in vitro* (2–6 days) for any of the measured parameters.

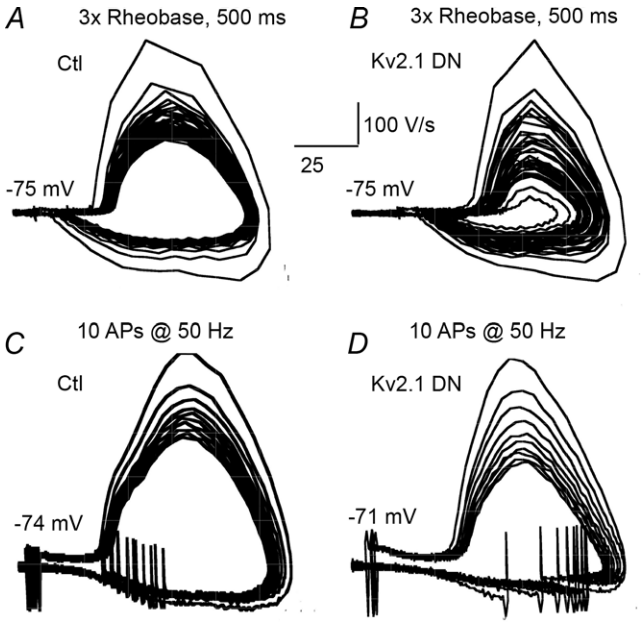

Figure 6. Phase relationships during repetitive firing in control and Kv2.1 DN cells
A and *B*, the trajectories of all APs during a 500 ms current injection at 3× rheobase. *C* and *D*, the trajectories of 10 spikes elicited by 10 suprathreshold, 5 ms current injections at 50 Hz. *A*, phase plot of APs during repetitive firing in a non-transfected cell. Note the relatively stable trajectories after the initial AP. *B*, phase plot of APs during repetitive firing in a Kv2.1 DN cell. Note the greater changes in trajectories of successive APs compared to those in *A*. There were greater changes in AP amplitude, voltage during ISIs and dV/dt in the Kv2.1 DN cells. *C*, non-transfected cell: phase plot of APs elicited by 10 stimuli (10 ms) at 50 Hz. The trajectories were more stable than during repetitive firing (e.g. *A*). *D*, Kv2.1 DN cell: phase plot of APs elicited by 10 stimuli (10 ms) at 50 Hz. The trajectories are stable and similar to the non-transfected cell in *C*.

Our most prominent finding was that reduction in functional expression with the Kv2.1 DN resulted in slower firing in response to a given input, with a reduced *f–I* slope (decreased gain: Fig. 4). These effects were robust whether stimulus amplitude is expressed as current or multiples of rheobase. Transfection of GFP alone or overexpression of the Kv2.1 WT did not result in significant differences in firing rate or *f–I* slope. Our findings are consistent with the observations of Johnston *et al.* (2008) in MNTB neurons and Du *et al.* (2000) in CA1 neurons, in that Kv2 channels play a role in regulating high frequency gain of firing and the effects of Kv2 manipulation are greatest for larger stimuli and at higher firing rates. In models proposed by Johnston *et al.* (2008) and Mohapatra *et al.* (2009), putative Kv2 current accumulates during ISIs, especially at higher firing rates, thereby promoting repetitive firing. Despite the fact that only a small fraction of the Kv2 channels activate with a single AP, their slow deactivation at ISI voltages allows Kv2 conductance to accumulate, especially at higher firing frequencies (Johnston *et al.* 2008). A

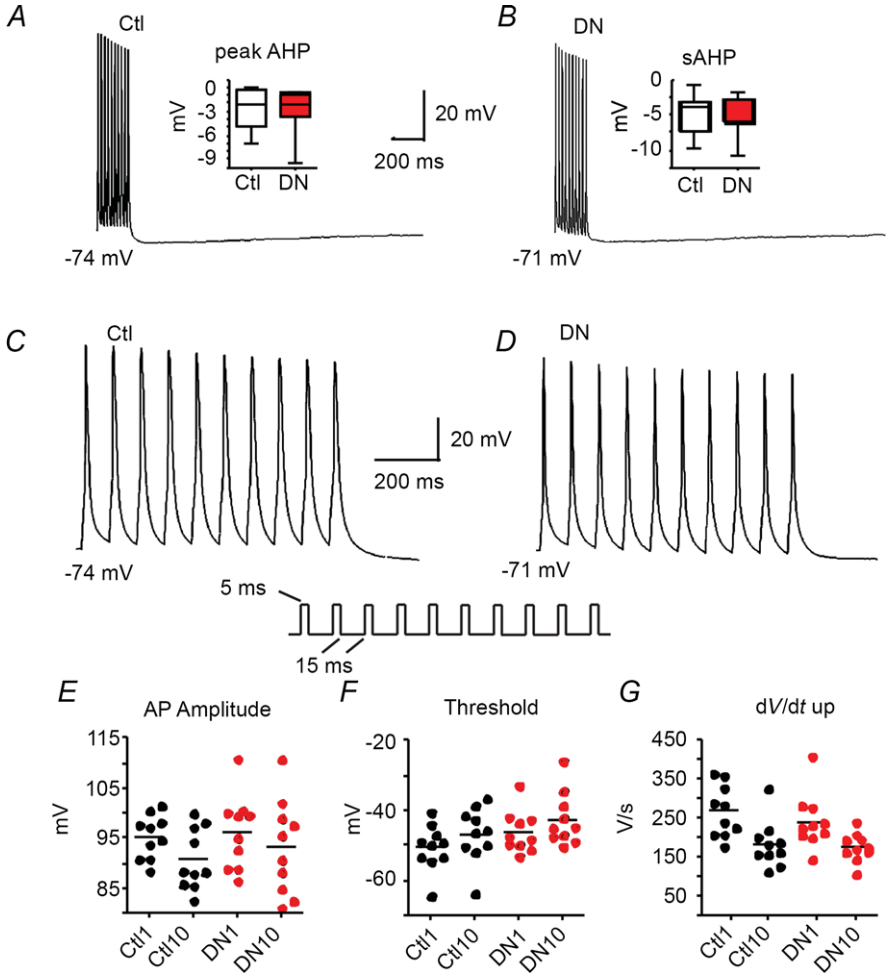

Figure 7. Trains of APs elicited at 50 Hz with 10 ms suprathreshold current injections
A, a train of APs in a non-transfected (Ctl) layer 5 pyramidal cell elicited by 10 APs at 50 Hz and shown with a slow time base to emphasize the afterhyperpolarization (AHP) following the spikes. *Inset*, box plot showing no differences in the peak AHP between non-transfected and Kv2.1 DN cells for this protocol (no significant differences). *B*, a train of APs elicited by 10 APs at 50 Hz in a cell transfected with the Kv2.1 DN in layer 5 of the same slice as cell in *A*. *Inset*, box plot showing no differences in the slow AHP (sAHP: measured at 500 ms) between non-transfected (Ctl) and Kv2.1 DN cells for this protocol (no significant differences). *C*, AP train shown in *A* except with expanded time scale. *Inset*, stimulus protocol. *D*, AP train shown in *B* except with expanded time scale. *E*, peak AP amplitude for the first and 10th AP compared between non-transfected (Ctl) and Kv2.1 DN cells. There were no differences between groups for the initial AP, the 10th AP or the changes between APs 1 and 10. *F*, AP voltage threshold for the first and 10th AP compared between non-transfected (Ctl) and Kv2.1 DN cells. There were no differences between groups for the initial AP, the 10th AP, or the changes between APs 1 and 10. *G*, AP rate of rise (d*V*/d*t* up) for the first and 10th AP compared between non-transfected (Ctl) and Kv2.1 DN cells. There were no differences between groups for the initial AP, the 10th AP, or the changes between APs 1 and 10.

frequency-dependent role for Kv2 (*Shab*) currents was also proposed at the *Drosphila* neuromuscular junction (Ueda & Wu, 2006).

Since K^+ channels in general reduce excitability, it is at first counter-intuitive that reduction in a Kv conductance should result in slower firing. Dynamic effects of K^+ conductances are more complicated, however, and there are precedents for such an action. Slowing of firing rate is also observed upon blocking Kv3.1 channels in neocortical GABAergic interneurons (Rudy *et al.* 1999; Rudy & McBain, 2001) or BK channels in hippocampal pyramidal neurons (Jaffe *et al.* 2011). Like Kv2 channels, Kv3.1 channels activate at depolarized potentials (high threshold), although with more rapid activation and deactivation kinetics *vs.* Kv2 channels (Rudy & McBain, 2001). BK channels are activated by both voltage and internal $[Ca^{2+}]_i$ and generally require an AP for activation. Thus, they are effectively high-threshold channels as well.

We found that the Kv2.1 DN group exhibited a failure to fire at earlier times and lower stimulation intensities compared to control cells (reduced dynamic range). Similarly, in the Malin and Nerbonne (2002) study of superior cervical ganglion neurons, the Kv2.2 DN reduced the percentage of tonic firing cells and increased the percentage of phasic and adapting cells. Notably, the phasic pattern was associated with a dramatic decline in spike amplitude and eventual spike failure. The proportions of different firing types did not change with Kv2.1 DN expression in that study. Conversely, in that study overexpression of Kv2.1 WT led to an increased proportion of tonic firing cells (and less decline in spike amplitude).

We also found significantly greater SFA in Kv2.1 DN cells *vs.* paired controls (Fig. 5). The spiking failures and greater reduction in dV/dt for the spike upstroke attained by Kv2.1 DN cells at higher firing rates leads us to favour the hypothesis that the slower firing and enhanced SFA may be due to increased inactivation of Na^+ channels. A similar conclusion was reached for MNTB cells (Johnston *et al.* 2008). They showed that potentials reached during ISIs approximated the steepest part of the steady-state inactivation curve for Na^+ currents in those cells. This relationship also holds for neocortical pyramidal neurons, where the half-inactivation voltage is ~ -60 mV (Huguenard *et al.* 1988). A slow cumulative inactivation process for Na^+ channels with repetitive spiking has been described in neocortical pyramidal cells, where it contributes to spike frequency adaptation and dynamic range for firing (Fleidervish *et al.* 1996). It is also possible that the enhanced SFA might be due to compensation for loss of Kv2 channels by enhanced Ca^{2+}-dependent K^+ currents that regulate SFA (Schwindt *et al.* 1988; Lorenzon and Foehring, 1993). Arguing against this possibility, we did not see larger AHPs after 10 spikes elicited at 50 Hz, where membrane potential recovers during ISIs and thus there is no sustained depolarization.

In neocortical pyramidal neurons, the slower firing rates in Kv2.1 DN cells were associated with a trend towards slightly more depolarized ISIs. In all experimental groups, the minimum membrane potential during the ISI was correlated with threshold, amplitude, spike HW and dV/dt (up and down) of the subsequent spike. Thus, in control cells, sustained depolarization during repetitive firing was associated with a trend toward higher threshold, lower amplitude, broader spikes and lower dV/dt of each successive AP during firing. These changes were progressive and approached a steady plateau level (cf. Fig. 5*C–F*). Cells transfected with GFP alone were nearly identical to non-transfected cells in these parameters. These relationships have *in vivo* relevance. For example, the relationship between dV/dt and spike threshold has been shown to enhance selectivity of somatosensory cortical neurons to specific sensory inputs *in vivo* (Wilent & Contreras, 2005).

When spiking was elicited by repeated short current injections from RMP at rates where there was no sustained depolarization between APs, AP parameters changed much less during the train and were almost identical in non-transfected and Kv2.1 DN cells (Fig. 7). These data suggest that Kv2 conductance during the ISI influences the properties of subsequent APs. In the Du *et al.* (2000) study, antisense treatment of cultured CA1 pyramidal cells to manipulate Kv2.1 channel expression did not result in changes in parameters of single APs elicited at low frequency but at higher stimulation rates (either with synaptic stimuli or mimicking ictal events with high extracellular K^+) they observed spike broadening.

We found that the reduced firing rate in the Kv2.1 DN cells was accompanied by a trends towards greater decline in spike height, greater elevation of spike threshold and greater spike widening during repetitive firing compared to matched control cells. The changes in the maximal dV/dt for spike repolarization reached statistical significance, consistent with reduced outward currents in the DN cells. The maximum dV/dt for the AP repolarization was also significantly reduced in the DN cells. These data suggest a reduced availability of Na^+ channels, consistent with cumulative Na^+ channel inactivation. Changes trended in the opposite direction for overexpression of Kv2.1 WT.

Consistent with a role for Kv2 channels in regulating the ISI, Na^+ availability and high frequency firing, Mohapatra *et al.* (2009) found that shifting the voltage dependence of activation of Kv2 channels in the hyperpolarized direction ($\sim$25 mV) by applying glutamate or DC current in cultured CA1 neurons led to greater Kv2 activation and resulted in slower firing to a given input. This effect was Ca^{2+}- and NMDA receptor-dependent and mediated by calcineurin. Thus, a similar functional effect can be generated by reduction in Kv2 expression without a change in voltage dependence (present results) or by shifting Kv2

from a 'high threshold' current to a 'low threshold' current (Mohapatra *et al.* 2009).

In conclusion, we found that 'high threshold' Kv2.1-containing channels are important regulators of ISIs, firing rate and SFA in neocortical pyramidal cells. Reduction of conductance from 'low threshold' (damping) potassium channels active in the subthreshold range typically results in lowered spike threshold and increased firing rate (e.g. Kv1: Guan *et al.* 2007*b*; Shu *et al.* 2007; Kv4: Yuan *et al.* 2005; Carrasquillo *et al.* 2012; Kv7: Hu *et al.* 2007; Guan *et al.* 2011*a*). In contrast, block of 'high threshold' Kv3 (Rudy & McBain, 2001) or BK (Gu *et al.* 2007) channels may lead to paradoxical slowing of firing as these channels allow rapid spike repolarization and/or removal of Na^+ inactivation. Kv2 channels are 'high threshold' but have relatively slow kinetics, and thus they have minimal effects on an isolated AP but their roles in controlling membrane potential during ISIs and preventing excessive inactivation of Na^+ channels become more significant with repeated spikes, especially at higher frequencies.

References

Abel HJ, Lee JC, Callaway JC & Foehring RC (2004). Relationships between intracellular calcium and afterhyperpolarizations in neocortical pyramidal neurons. *J Neurophysiol* **91**, 324–335.

Archer SL, Souil E, Dinh-Xuan AT, Schremmer B, Mercier JC, El Yaagoubi A, Nguyen-Huu L, Reeve HL & Hampl V (1998). Molecular identification of the role of voltage-gated K^+ channels, Kv1.5 and Kv2.1, in hypoxic pulmonary vasoconstriction and control of resting membrane potential in rat pulmonary artery myocytes. *J Clin Invest* **101**, 2319–2330.

Bean BP (2007). The action potential in mammalian central neurons. *Nat Rev Neurosci* **8**, 451–465.

Blaine JT & Ribera AB (2001). Kv2 channels form delayed-rectifier potassium channels *in situ*. *J Neurosci* **21**, 1473–1480.

Carrasquillo Y, Burkhalter A & Nerbonne JM (2012). A-type K^+ channels encoded by Kv4.2, Kv4.3 and Kv1.4 differentially regulate intrinsic excitability of cortical pyramidal neurons. *J Physiol* **590**, 3877–3890.

Coetzee WA, Amarillo Y, Chiu J, Chow A, Lau D, McCormack T, Moreno H, Nadal MS, Ozaita A, Pountney D, Saganich M, Vega-Saenz de Miera E & Rudy B (1999). Molecular diversity of K^+ channels. *Ann N Y Acad Sci* **868**, 233–285.

Dodt HU & Zieglgänsberger W (1990). Visualizing unstained neurons in living brain slices by infrared DIC-videomicroscopy. *Brain Res* **537**, 333–336.

Drummond GB (2009). Reporting ethical matters in the *Journal of Physiology*: standards and advice. *J Physiol* **587**, 713–719.

Du J, Haak LL, Phillips-Tansey E, Russell JT & McBain CJ (2000). Frequency-dependent regulation of rat hippocampal somato-dendritic excitability by the K^+ channel subunit Kv2.1. *J Physiol* **522**, 19–31.

Dyhrfjeld-Johnsen J, Berdichevsky Y, Swiercz W, Sabolek H & Staley KJ (2010). Interictal spikes precede ictal discharges in an organotypic hippocampal slice culture model of epileptogenesis. *J Clin Neurophysiol* **27**, 418–424.

Escoubas P, Diochot S, Célérier ML, Nakajima T & Lazdunski M (2002). Novel tarantula toxins for subtypes of voltage-dependent potassium channels in the Kv2 and Kv4 subfamilies. *Mol Pharmacol* **62**, 48–57.

Fleidervish IA, Friedman A & Gutnick MJ (1996). Slow inactivation of Na^+ current and slow cumulative spike adaptation in mouse and guinea-pig neocortical neurons in slices. *J Physiol* **493**, 83–97.

Foehring RC, Guan D, Toleman T & Cantrell AR (2011). An organotypic slice preparation of neocortex for whole cell recording from transfected neurons. *J Vis Exp* **3**, pii: 2600.

Fox PD, Loftus RJ & Tamkun MM (2013). Regulation of Kv2.1 K^+ conductance by cell surface channel density. *J Neurosci* **33**, 1259–1270.

Gu N, Vervaeke K & Storm JF (2007). BK potassium channels facilitate high-frequency firing and cause early spike frequency adaptation in rat CA1 hippocampal pyramidal cells. *J Physiol* **580**, 859–882.

Guan D, Higgs MH, Horton, LR, Spain WJ & Foehring RC (2011*a*). Contributions of Kv7-mediated potassium current to sub- and suprathreshold responses of rat layer II/III neocortical pyramidal neurons. *J Neurophysiol*, **106**, 1722–1733.

Guan D, Horton LR, Armstrong WA & Foehring RC (2011*b*). Postnatal development of A-type and Kv1- and Kv2-mediated potassium channel currents in neocortical pyramidal neurons. *J Neurophysiol* **105**, 2976–2988.

Guan D, Lee JC-F, Higgs M, Spain WJ, Armstrong WE & Foehring RC (2007*a*). Functional roles of Kv1 containing channels in neocortical pyramidal neurons. *J Neurophysiol* **97**, 1931–1940.

Guan D, Lee JC, Tkatch T, Surmeier DJ, Armstrong WE & Foehring RC (2006). Expression and biophysical properties of Kv1 channels in supragranular neocortical pyramidal neurones. *J Physiol* **571**, 371–389.

Guan D, Tkatch T, Surmeier DJ, Armstrong WE, and Foehring RC (2007*b*). Kv2 subunits underlie slowly inactivating potassium current in rat neocortical pyramidal neurons. *J Physiol* **581**, 941–960.

Henze DA & Buzsaki G (2001). Action potential threshold of hippocampal pyramidal cells is increased by recent spiking activity. *Neuroscience* **105**, 121–130.

Hermanstyne TO, Kihira Y, Misono K, Deitchler A, Yanagawa Y & Misonou H (2010). Immunolocalization of the voltage-gated potassium channel Kv2.2 in GABAergic neurons of the basal forebrain of rats and mice. *J Comp Neurol* **518**, 4298–4310.

Higgs, MH, Slee SJ & Spain WJ (2006). Diversity of gain modulation by noise in neocortical neurons: regulation by the slow afterhyperpolarization conductance. *J Neurosci* **26**, 8787–8799.

Higgs, MH & Spain WJ (2011). Kv1 channels control spike threshold dynamics and spike timing in cortical pyramidal neurons. *J Physiol* **589**, 5125–5142.

Hu H, Vervaeke K & Storm JF (2007). M-channels (Kv7/KCNQ channels) that regulate synaptic integration, excitability, and spike pattern of CA1 pyramidal cells are located in the perisomatic region. *J Neurosci* **27**, 1853–1867.

Huguenard JR, Hamill OP & Prince DA (1988). Developmental changes in Na^+ conductances in rat neocortical neurons: appearance of a slowly inactivating component. *J Neurophysiol* **59**, 778–795.

Hwang PM, Fotuhi M, Bredt DS, Cunningham AM & Snyder SH (1993). Contrasting immunohistochemical localizations in rat brain of two novel K^+ channels of the Shab subfamily. *J Neurosci* **13**, 1569–1576.

Jaffe DB, Wang B & Brenner R (2011). Shaping of action potentials by type I and type II large-conductance Ca^{2+}-activated K^+ channels. *Neuroscience* **192**, 205–218.

Johnston J, Griffin SJ, Baker C, Skrzypiec A, Chernova T & Forsythe ID (2008). Initial segment Kv2.2 channels mediate a slow delayed rectifier and maintain high frequency action potential firing in medial nucleus of the trapezoid body neurons. *J Physiol* **86**, 3493–3509.

Kang J, Huguenard JR & Prince, DA (2000). Voltage-gated potassium channels activated during action potentials in layer V neocortical pyramidal neurons. *J Neurophysiol* **83**, 70–80.

Kihira Y, Hermanstyne TO & Misonou H (2010). Formation of heteromeric Kv2 channels in mammalian brain neurons. *J Biol Chem* **285**, 15048–15055.

Kulkarni RS, Zorn LJ, Anantharam V, Bayley H & Treistman SN (1996). Inhibitory effects of ketamine and halothane on recombinant potassium channels from mammalian brain. *Anesthesiology* **84**, 900–909.

Locke RE & Nerbonne JM (1997). Role of voltage-gated K^+ currents in mediating the regular-spiking phenotype of callosal-projecting rat visual cortical neurons. *J Neurophysiol* **78**, 2321–2335.

Lorenzon NM & Foehring RC (1993). The ontogeny of repetitive firing and its modulation by norepinephrine in rat neocortical neurons. *Brain Res Dev Brain Res* **73**, 213–223.

Lu Y, Hanna ST, Tang G & Wang R (2002). Contributions of Kv1.2, Kv1.5 and Kv2.1 subunits to the native delayed rectifier K^+ current in rat mesenteric artery smooth muscle cells. *Life Sci* **71**, 1465–1473.

Madeja M (2000). Do neurons have a reserve of sodium channels for the generation of action potentials? A study on acutely isolated CA1 neurons from the guinea-pig hippocampus. *Eur J Neurosci* **12**, 1–7.

Madison DV & Nicoll RA (1984). Control of the repetitive discharge of rat CA 1 pyramidal neurones *in vitro*. *J Physiol* **354**, 319–331.

Malin SA & Nerbonne JM (2002). Delayed rectifier K^+ currents, IK, are encoded by Kv2 a-subunits and regulate tonic firing in mammalian sympathetic neurons. *J Neurosci* **22**, 10094–10105.

McCormick DA & Prince DA. (1987). Post-natal development of electrophysiological properties of rat cerebral cortical pyramidal neurones. *J Physiol* **393**, 743–762.

Miller MN, Okaty BW, Nelson SB. (2008). Region-specific spike-frequency acceleration in layer 5 pyramidal neurons mediated by Kv1 subunits. *J Neurosci.* **28**, 13716–13726.

Misonou H, Mohapatra DP, Menegola M & Trimmer JS (2005*a*). Calcium- and metabolic state-dependent modulation of the voltage-dependent Kv2.1 channel regulates neuronal excitability in response to ischemia. *J Neurosci* **25**, 11184–11193.

Misonou H, Mohapatra DP, Park EW, Leung V, Zhen D, Misonou K, Anderson AE & Trimmer JS (2004). Regulation of ion channel localization and phosphorylation by neuronal activity. *Nat Neurosci* **7**, 711–718.

Misonou H, Mohapatra DP & Trimmer JS (2005*b*). Kv2.1: a voltage-gated K^+ channel critical to dynamic control of neuronal excitability. *Neurotoxicology* **26**, 743–752.

Mohapatra DP, Misonou H, Pan SJ, Held JE, Surmeier DJ & Trimmer JS (2009). Regulation of intrinsic excitability in hippocampal neurons by activity-dependent modulation of the KV2.1 potassium channel. *Channels* **3**, 46–56.

Murakoshi H & Trimmer JS (1999). Identification of the Kv2.1 K^+ channel as a major component of the delayed rectifier K^+ current in rat hippocampal neurons. *J Neurosci* **19**, 1728–1735.

Nataraj K, Le Roux N, NAhmani M, Lefort S & Turrigiano G (2010). Visual deprivation suppresses L5 pyramidal neuron excitability by preventing the induction of intrinsic plasticity. *Neuron* **68**, 750–762.

Norris AJ & Nerbonne JM (2010). Molecular dissection of I_A in cortical pyramidal neurons reveals three distinct components encoded by Kv4.2, Kv4.3, and Kv1.4 a-subunits. *J Neurosci* **30**, 5092–5101.

O'Connell KM, Loftus R & Tamkun MM (2010). Localization-dependent activity of the Kv2.1 delayed-rectifier K^+ channel. *Proc Natl Acad Sci U S A* **107**, 12351–12356.

Park KS, Yang JW, Seikel E & Trimmer JS (2008). Potassium channel phosphorylation in excitable cells: providing dynamic functional variability to a diverse family of ion channels. *Physiology* **23**, 49–57.

Pal S, Hartnett KA, Nerbonne JM, Levitan ES & Aizenman, E (2003). Mediation of neuronal apoptosis by Kv2.1-encoded potassium channels. *J Neurosci* **23**, 4798–4802.

Pineda JC, Galarraga E & Foehring RC (1999). Different Ca^{2+} source for slow AHP in completely adapting and repetitive firing pyramidal neurons. *Neuroreport* **10**, 1951–1956.

Rudy B, Chow A, Lau D, Amarillo Y, Ozaita A, Saganich M, Moreno H, Nadal MS, Hernandez-Pineda R, Hernandez-Cruz A, Erisir A, Leonard C & Vega-Saenz de Miera E (1999). Contributions of Kv3 channels to neuronal excitability. *Ann N Y Acad Sci* **868**, 304–343.

Rudy B & McBain CJ (2001). Kv3 channels: voltage-gated K^+ channels designed for high-frequency repetitive firing. *Trends Neurosci* **24**, 517–526.

Stoppini L, Buchs PA & Muller D (1991). A simple method for organotypic cultures of nervous tissue. *J Neurosci Methods* **37**, 173–182.

Stuart GJ, Dodt HU & Sakmann B (1993). Patch-clamp recordings from the soma and dendrites of neurons in brain slices using infrared video microscopy. *Pflugers Arch* **423**, 511–518.

Sarmiere PD, Weigle CM & Tamkun MM (2008). The Kv2.1 K^+ channel targets to the axon initial segment of hippocampal and cortical neurons in culture and *in situ*. *BMC Neurosci* **9**, 112.

Schwindt PC, Spain WJ, Foehring RC, Chubb MC & Crill WE (1988). Slow conductances in neurons from cat sensorimotor cortex *in vitro*: their modulation by neurontransmitters and their role in slow excitability changes. *J Neurophysiol* **59**, 450–467.

Shu Y, Yu Y, Yang J & McCormick DA (2007). Selective control of cortical axonal spikes by a slowly inactivating K^+ current. *Proc Natl Acad Sci U S A* **104**, 11453–11458.

Singer-Lahat D, Sheinin A, Chikvashvili D, Tsuk S, Greitzer D, Friedrich R, Feinshreiber L, Ashery U, Benveniste M, Levitan ES & Lotan I (2007). K^+ channel facilitation of exocytosis by dynamic interaction with syntaxin. *J Neurosci* **27**, 1651–1658.

Surmeier DJ & Foehring RC (2004). A mechanism for homeostatic plasticity. *Nature Neurosci* **7**, 691–692.

Trimmer JS (1991). Immunological identification and characterization of a delayed rectifier K^+ channel polypeptide in rat brain. *Proc Natl Acad Sci U S A* **88**, 10764–10768.

Tukey JW (1977). Exploratory data analysis. Reading, MA: Addison–Wesley.

Ueda A & Wu CF (2006). Distinct frequency-dependent regulation of nerve terminal excitability and synaptic transmission by I_A and I_K potassium channels revealed by *Drosophila Shaker* and *Shab* mutations. *J Neurosci* **26**, 6238–6248.

Wilent WB & Contreras D (2005). Stimulus-dependent changes in spike threshold enhance feature selectivity in rat barrel cortex neurons. *J Neurosci* **25**, 2983–2991.

Yuan W, Burkhalter A & Nerbonne JM (2005). Functional role of the fast transient outward K^+ current I_A in pyramidal neurons in (rat) primary visual cortex. *J Neurosci* **25**, 9185–9194.

Xu H, Barry DM, Li H, Brunet S, Guo W & Nerbonne JM (1999). Attenuation of the slow component of delayed rectification, action potential prolongation, and triggered activity in mice expressing a dominant-negative Kv2 α subunit. *Circ Res* **85**, 623–633.

Additional information

Competing interests

There were no competing interests to report for any of the authors.

Author contributions

The transfections, cultures, and recordings were done in LDr. Foehring's lab by Drs. Guan and Foehring, who also analyzed and interpreted these data. The immunocytochemistry was done in Dr. Armstrong's lab. All authors contributed to the conception and design of the experiments. The article was drafted by Dr. Foehring and edited by all of the authors. All authors approved the final version of the manuscript, all persons designated as authors qualify for authorship, and all those who qualify for authorship are listed.

Funding

This work was funded by NIH grant NS44163 (to RCF).

Acknowledgements

We especially wish to thank Rodrigo Andrade for his help in developing the methodology for organotypic slice culture and biolistic transfection in our lab. Excellent technical assistance was provided by Angela Cantrell, Tara Toleman, Mayumi Sakuraba, Roy Horton and Rebecca Foehring.